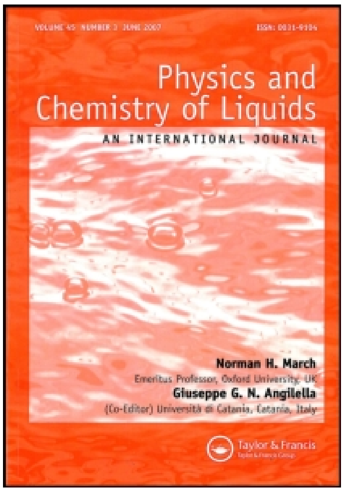

Physics and Chemistry of Liquids
Publication details, including instructions for authors and subscription information:
http://www.informaworld.com/smpp/title~content=t713646857

Melting and related precursor cooperative phenomena in chemically bonded assemblies

N. H. March[a][b]
[a] Donostia International Physics Centre, San Sebastian, Spain, Oxford University, Oxford, England [b] The Abdus Salam International Centre for Theoretical Physics, Trieste, Italy

To cite this Article March, N. H.(2006) 'Melting and related precursor cooperative phenomena in chemically bonded assemblies', Physics and Chemistry of Liquids, 44: 5, 477 — 492

To link to this Article: DOI: 10.1080/00319100500424209

URL: http://dx.doi.org/10.1080/00319100500424209

Physics and Chemistry of Liquids
Vol. 44, No. 5, October 2006, 477–492

Taylor & Francis
Taylor & Francis Group

Review

Melting and related precursor cooperative phenomena in chemically bonded assemblies

N. H. MARCH

Donostia International Physics Centre, San Sebastian, Spain,
Oxford University, Oxford, England and
The Abdus Salam International Centre for Theoretical Physics, Trieste, Italy

(*Received 20 January 2005*)

A number of experimental studies of condensed matter assemblies with different types of chemical bonding will provide the focus of this work. Condensed compounds $X(CH_3)_4$, with $X = C$, Si or Ge, are the first of such assemblies; two phase boundaries in the pressure–temperature plane being studied: melting and a solid phase boundary heralding orientational disordering of molecules still however on a lattice. Secondly, directionally bonded *d*-electron transition metals such as Ni, Pd and Nb will be treated. Here, melting is the main focus, but the precursor transition is now the separation of a high-temperature ductile solid from a lower temperature mechanically brittle phase. A dislocation-mediated model of these transitions is discussed, leading into the third area of covalently bonded solids graphite and silicon. Here topological defect models again provide the focus; both dislocations and rotation-dislocations now being invoked. Some qualitative suggestions are made to interpret the melting curve of graphite subjected to high pressure.

Keywords: Melting; Point and extended defects; Precursor transitions

1. Background

Melting models and/or criteria have a long history and, naturally enough, have often focussed on simple crystals formed from *almost spherical* building blocks, condensed argon being a prime example.

Here our aim is different and the focus of the present study will be on chemically bonded assemblies. We have chosen three specific areas by way of illustration, namely:

- (I) Melting and a related lower temperature phase boundary of solid $X(CH_3)_4$: $X = C$, Si, Ge as a function of pressure.
- (II) Melting and associated physical properties in *d*-electron transition metals, examples referred to including the body-centred-cubic (bcc) element Nb and the face-centred-cubic structures of Pd and Ni and
- (III) Melting transition in graphite, and quite briefly also in silicon.

Physics and Chemistry of Liquids
ISSN 0031-9104 print/ISSN 1029-0451 online
DOI: 10.1080/00319100500424209

As to the *related precursor cooperative phenomena* referred to in the title of this Review, in area I this concerns the phase boundary in solid $X(CH_3)_4$ which marks the separation, prior to melting, of a low-temperature orientationally ordered molecular phase, say at a given pressure, from a phase characterized by orientational disorder, with in both cases however the molecules still attached to the sites of a crystal lattice.

In area II, the precursor transition to melting, say in the bcc transition metal Nb referred to above, is the so-called brittle-to-ductile transition (BDT). A *rule of thumb* sometimes used by materials scientists, and detailed further below, at atmospheric pressure, relates grossly the temperature of this transition denoted by T_{BDT}, to a fraction of the melting temperature T_m.

As to the third area, silicon is possibly the elemental solid in which the BDT has been most carefully studied experimentally. However, although a BDT seems not to have been observed at the time of writing in graphite, for presentational purposes a single graphene layer consisting of hexagons of C atoms with sp^2 hybridization provides a most useful starting point.

With this background, let us turn immediately to area I. After some phenomenology, which can in fact be traced back to the very early order-disorder model of Bragg and Williams, qualitative contact will then be made with prominent features of the measured pressure–temperature (p, T) phase diagram of condensed $C(CH_3)_4$.

2. Melting curve under pressure related to phase boundary heralding orientational disorder of $X(CH_3)_4$ molecules in these solid compounds with $X = $ C, Si or Ge

To gain insight into the behaviour of molecular solids under externally applied pressure, Tozzini *et al.* [1] have previously discussed orientational disorder and melting, using phenomenology plus modelling, with respect to solid halogens and H_2. Here our focus, as indicated above, will be the phase diagram of condensed $X(CH_3)_4$. Stimulation was afforded by the study of Siringo [2], in which a *d*-dimensional lattice model, incorporating some degree of frustration and therefore capable of treating some properties associated with molecular orientation in solids was proposed. Though Siringo's work has quite fundamental interest and for $d = 2$ is equivalent to the standard two-dimensional Ising model, we shall here follow Tozzini *et al.* [1] and utilize the phenomenology laid down by Pople and Karasz [3: see also extension in refs [4] and [5]]. We note that the Pople-Karasz (PK) phenomenology generalizes the Lennard-Jones and Devonshire [6] approach to melting, based on the Bragg-Williams approximation, to embrace the possibility of orientational disordering. Following PK, who restricted their model to but two possible molecular orientations, separated by a suitable energy barrier (for n orientations with $n > 2$, see ref [5]) we summarize using the notation employed in the book by Ubbelohde [7], the phenomenological equations for the two *order parameters* Q and S, namely

$$\frac{1}{2Q-1}\ln\left[\frac{Q}{1-Q}\right] = L[1 - 2S(1-S)y] \tag{2.1}$$

and

$$\frac{1}{2S-1}\ln\left[\frac{S}{1-S}\right] = 2Ly[1-2Q+2Q^2], \tag{2.2}$$

Q referring to positional order/disorder with S the corresponding orientational parameter. These two equations are characterized by the dimensionless quantities L and y defined by [1]

$$L = ZW/2k_BT \tag{2.3}$$

and

$$y = Z'W'/ZW. \tag{2.4}$$

Putting y to zero in equation (2.2) the melting model of Lennard-Jones and Devonshire [6] is recovered, with the thermal energy k_BT_m corresponding to the melting temperature T_m then determined solely in terms of the energy ZW which, roughly speaking, is a diffusion energy. The other energy parameter $Z'W'$ constitutes the barrier height separating different orientational arrangements: the latter quantity being the essential new feature proposed by PK. Figure 1, redrawn from Tozzini *et al.* [1], shows the reduced melting temperature $t_m = 2k_B/ZW$ (upper line) and reduced orientational disordering temperature $t_c = 2k_BT_c/ZW$ (lower line) *versus* the ratio y defined in equation (2.4). The two lines are seen to meet at $y_0 \simeq 0.595$ and they coincide for $y > y_0$. This diagram illustrates the *precursor collective phenomenon*: in this case the phase boundary separating the orientationally ordered and disordered phases (reduced temperature $t_c(y)$ in figure 1). In particular, figure 1 depicts the way in which this lower temperature transition is interconnected with the melting transition.

Though in ref [1], modest contact was established with solid H_2 and the halogens, it has subsequently come to the author's attention that very relevant proton magnetic resonance (PMR) experiments are recorded in the older literature for the solid tetramethyls already referred to. We refer here especially to the study [8] of neopentane, $C(CH_3)_4$. Since PMR experiments measure directly appropriate energy barriers, which are in turn related to the above phenomenological parameters $Z'W'$ and ZW entering equations (2.1)–(2.4), one can estimate the parameter y for $C(CH_3)_4$ as 0.11. Also the melting temperature for this compound is known to be 256 K. The predictions of the PK phenomenology are then in qualitative agreement with the PMR measurements for this material. However, there is one matter of some substance which must be mentioned here. For the above parameter value of y, the PK phenomenology predicts the re-orientational transition to be second order, which disagrees with the experimental results of $C(CH_3)_4$ which exhibits a first-order transition. It would therefore be of obvious interest if, for the parameters of this material one could transcend the PK phenomenology by working out the predictions, say of the Siringo Hamiltonian [2].

Figure 1 is qualitatively in accord with the two corresponding phase boundaries determined as a function of pressure for condensed N_2, the experimental curves being given in figure 1 of ref [8]. For earlier theoretical work on solid N_2 the reader should consult the study of LeSar [9].

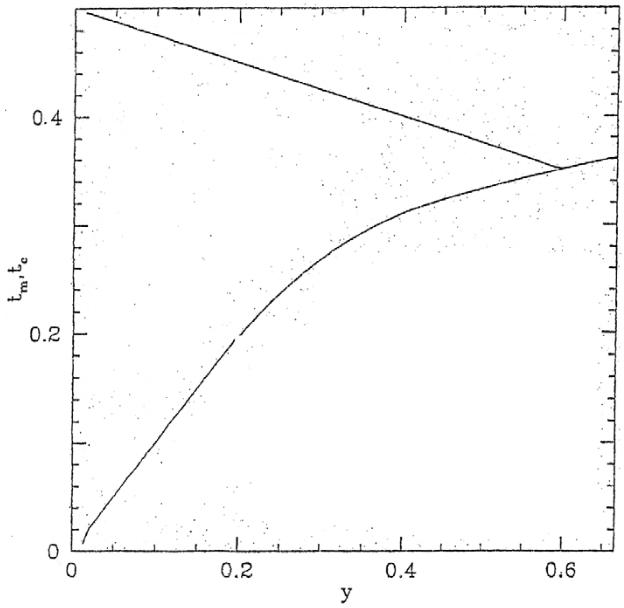

Figure 1. Reduced melting temperature $t_m = 2k_BT_m/ZW$ (upper line) and reduced orientational order/disorder temperature $t_c = 2k_BT_c/ZW$ resulting from solutions of the simultaneous equations (2.1) and (2.2). The dimensionless independent variable in this plot is y defined in equation (2.4). This measures the energy barrier to orientational change in units of a characteristic activation energy for diffusion, in the phenomenology adopted. [Redrawn from Tozzini *et al.* [1].]

3. Melting and related phase boundaries in directionally bonded *d*-electron transition metals

Motivated by the pioneering work of Kirkwood and Monroe [10], a quantitative statistical mechanical theory of freezing [11–14] now exists. Notwithstanding this, there has been a recent resurgence of interest in models, and also criteria, which aim to provide insight into the regularities exhibited by empirical melting temperatures: here our prime interest is with the *d*-electron bonded transition metals.

Quite recent contributions of this kind have been made by Kleinert and Jiang (KJ) [15], Lawson [16] and Burakovsky and co-workers [17,18]. Here we shall report on the subsequent study of Matthai and March [19] who have emphasized especially the common features shared by the treatments of KJ and Burakovsky *et al.*

The most important of these shared features is that the melting transition is assumed to be dislocation-mediated. Both KJ and Burakovsky *et al.*, as stressed by Matthai and March [19], are led to a result for the thermal T_m having the general shape.

$$k_BT_m = \Omega F\,(\text{elastic constants})\; S. \tag{3.1}$$

In equation (3.1), Ω denotes the atomic volume, while S is a structure-dependent factor. Matthai and March examined S for the *d*-bonded bcc and fcc transition

Table 1. Experimental data for three directionally bonded transition metals (after [19]).

Element	G_r (GPa)	G_m (GPa)	Ω (Å^3)	L_m (eV atom^{-1})	T_m (K)	$k_BT_m/G_m\Omega$	$k_BT_m/G_r\Omega$
Ni	85.8	41.8	10.95	0.183	1726	5.2	2.5
Pd	48.0	37.2	14.71	0.179	1825	4.6	3.6
Nb	37.6	35.0	18.01	0.279	2741	6.0	5.6

G_r and G_m denote respectively room temperature and (just below) melting temperature shear moduli. Ω is atomic volume, T_m melting temperature and L_m is latent heat of fusion.

metals and their findings will be summarized below. However, their study assumed the specific, and very simple, form of the function F adopted by Burakovsky and co-workers. Though their assumptions are somewhat oversimplified compared with those of KJ, they are thereby led to the intuitively appealing result

$$k_BT_m = \Omega G S_{LA} \tag{3.2}$$

where G is the shear modulus, while S_{LA} denotes the structure-dependent part given by the Los Alamos (LA) group of Burakovsky *et al.* Table 1, extracted from the work of Matthai and March, shows experimental results for the ratio $k_BT_m/G\Omega$ for some transition metal elements with highly directional bonding, with G taken from experiment both at room temperature (G_r) and just below the melting temperature (G_m). Matthai and March [18] propose, for a wider class of 13 elemental metals, that $S_{LA} = [5 \pm 0.4]$ for fcc structures and $[7 \pm 1]$ for bcc structures.

Burakovsky *et al.* [17] have also used the dislocation-mediated model to estimate the enthalpy of such an approach, and hence to obtain the latent heat of fusion L_m as an enthalpy difference. The very specific result in their equation (45) relates L_m directly to the melting temperature T_m times a structure-dependent factor characterized solely by the local coordination number. As Matthai and March [19] point out, eliminating the structure-dependent factor yields

$$\frac{L_m}{G\Omega} = \text{constant}, \tag{3.3}$$

where the right-hand side is now structure independent. Experimental data for the latent heat L_m is also recorded in table 1. Figure 2, redrawn from Matthai and March [19], shows a plot of the ratio $L_m/G\Omega$ entering equation (3.3) *versus* atomic number Z for the wider class of 13 elements, including the 5 bcc alkali metals. With the shear modulus G taken from experiment at (just below) the melting temperature T_m, the ratio in equation (3.3) has a range of values falling in a narrow band to within 20% of the mean. Matthai and March note that when the room temperature values of G are employed, there is much more scatter.

3.1. *Relation of k_BT_m to monovacancy formation energy E^f_{IV}*

Materials scientists have, over some decades, frequently recorded an empirical correlation between the thermal energy at melting, k_BT_m, and the monovacancy formation energy E^f_{IV}. The rule of thumb emerging from such discussions is

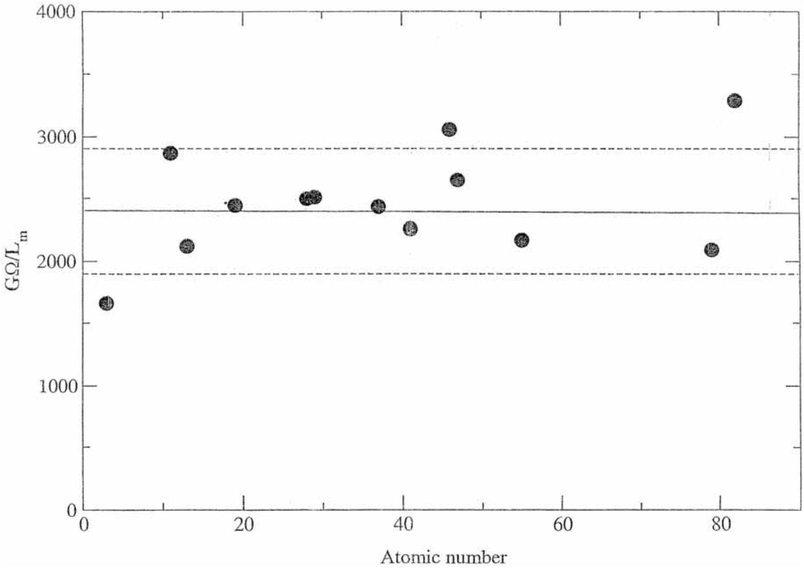

Figure 2. Displays the ratio $G\Omega/L_m$ *versus* atomic number where G, the shear modulus is taken from experiment just below melting, Ω is the atomic volume and L_m is the measured latent heat of fusion. [Redrawn from Matthai and March [19].].

that $E^f_{IV}/k_BT_m \sim 10$. In contrast with the dislocation-mediated phase transition discussed above, point defect correlations lack any such underlying mechanism, as no experimental evidence is found for any major build-up of the (small) monovacancy concentration as the melting temperature T_m is approached. Therefore, first-principles theories of such a correlation between E^f_{IV} and k_BT_m have appealed to an assumed force field. To take a specific example, Bhatia and March (BM) [20] have utilized, for close-packed solids, a pair-potential formulation by Minchin *et al.* [21] for E^f_{IV}. Although the BM treatment is most applicable for solid Ar already mentioned above, it leads to a quite clear cut prediction for the ratio E^f_{IV}/k_BT_m. In particular, BM observed that the ratio in their pair potential framework is given by

$$\frac{E_V}{k_BT_m} + \frac{1}{2}\frac{B\Omega}{k_BT_m} = -\left[\frac{c(r=0)+2}{2}\right]_{T_m} \tag{3.4}$$

where B is the bulk modulus while $c(r)$ is the Ornstein-Zernike direct correlation function [22]. Its Fourier transform, $\tilde{c}(q)$ say, is related to the liquid structure factor $S(q)$ by [22]

$$\tilde{c}(q) = [S(q) - 1]/S(q). \tag{3.5}$$

The writer has argued, using work of Johnson [23], which transcends the pair potential description employed in the model of Bhatia and March [20] yielding equation (3.4), that the bulk modulus B should be replaced by the shear modulus when pair potentials are replaced by a glue model [24]. A brief discussion is added in Appendix 3.1.

The correlation between $k_B T_m$ and $G\Omega$, via a structure-dependent factor, when combined with Johnson's work assuming specifically a face-centred cubic structure, is consistent with the approximate correlation $E^f_{IV}/k_B T_m =$ constant.

3.2. *Brittle-to-ductile transition in directionally bonded d-electron metals*

Materials scientists over the last decade have shown considerable interest in the interpretation of the brittle-to-ductile transition, prompted at least in part by the important study of Khantha, Pope and Vitek [25; referred to below as KPV]. These authors proposed to adapt the Kosterlitz-Thouless instability [26,27] to treat the BDT, this instability being related to the unbinding of dislocation pairs. While some changes in their original study are called for [28,29], the discussion of Sun, Hassledine and Hirsch [30, SHH below] validates some, though not all, of the features of the KPV proposal.

What we stress, first of all, is that KPV refer to a *rule of thumb* that in materials with low initial dislocation density, the transition temperature T_{BDT} is roughly one-half of the melting temperature T_m. In SHH [30], referring to Ni as an example they consider, T_{BDT} is quoted as 895 K, to be compared with the melting temperature T_m given in table 1 above as 1726 K. It is relevant to note here that the Curie temperature of Ni is 627 K; i.e. below T_{BDT}.

Next, it is to be noted that SHH develop a cooperative mechanism for the nucleation of subcritical shear loops driven by image stress and configurational entropy. Use of this mechanism leads them to correlate T_{BDT} with the shear modulus G. Invoking then the dislocation-mediated melting formula (3.2), one has the gist of the sought-after correlation between T_{BDT} and T_m. Related models are analysed somewhat further in Appendix 3.2.

Though these discussions (see also [28] and [29]) are evidently yielding further insight into the BDT, Klein and March [31] have very recently emphasized the central importance of *rotation-dislocations* or, as alternatively termed, *disclinations* for the BDT. This leads naturally into the third area of chemically bonded materials to be discussed, namely graphite and silicon.

4. Melting and brittle-to-ductile transition (BDT) in covalently bonded crystals: graphite and silicon

4.1. *Rotation-dislocations as the 'universal ingredient' of the BDT*

Since the melting temperature T_m and the BDT temperature T_{BDT} have been argued in section 3 above to be intimately correlated, let us introduce immediately the basic reason why Klein and March [31] have focussed very recently on the rotation-dislocation, or disclination, as the 'universal ingredient' in the BDT.

Together with Langer and Pechenick [32], who do not however mention disclinations, Klein and March [31] first exclude dislocations (translational) themselves as the 'universal ingredient' since the BDT is found experimentally in amorphous materials as well as in many crystalline solids.

Table 2. Ratio of experimental values of monovacancy formation energy E^f_{IV} to measured melting temperature T_m for eight close-packed metals (after [19]).

Element	E^f_{IV} (eV)	T_m (K)	E^f_{IV}/k_BT_m
Cu	1.31	1356	11.2
Ag	1.11	1234	10.4
Au	0.94	1336	8.2
Mg	0.89	923	11.2
Zn	0.54	693	9.0
Cd	0.36	594	7.6
Al	0.66	933	8.2
Pb	0.50	601	9.7

For these close-packed metals, experiment yields $E^f_{IV}/k_BT_m = 9.4 \pm 1.8$.

4.2. *Topological defects in graphite*

The above experimental findings have motivated Klein and March [31] to focus first on the chemical bonding (sp^2) structure of graphite. They develop a picture there relating to rotation-dislocations in terms of a perfect two-dimensional hexagonal layer of C atoms (graphene) being thermally excited such that both pentagonal and heptagonal *defects* are formed at elevated temperatures.

However, before expanding further on these arguments, it should be made clear that, to date, in graphite itself, the writer is presently unaware of any experimental observation of a BDT in this material. This is in contrast to Si, where the BDT is well-established, as discussed by KPV and SHH. It is fair to add, in the above context, first of all, that, as KPV write, ‘the ... BDT is a classic phenomenon exhibited by almost all materials ... ’. Secondly, the present absence of observation of a BDT in graphite may be due to its very high melting temperature $T_m > 4000$ K, which will be discussed a little further later. The *rules* relating T_{BDT} and T_m quoted above (see also Appendix 3.2) then strongly suggest that T_{BDT} may well lie between 2500 and 3000 K in graphite at atmospheric pressure (if indeed it exists in the material!).

4.3. *Chemical interpretation of topological defects in graphene: pentagons and heptagons at elevated temperatures*

Returning to thermally generated defects, with graphite being built up from appropriately stacked hexagonal planes of C atoms with interplanar van der Waals forces, Klein and March [31: see also Klein [33,34]] have made a comprehensive characterization of different possible rotation-dislocations in a single graphite sheet. There it is pointed out that the picture put forward can be presented in terms of dislocations first developing below T_{BDT} and then dissociating into rotation-dislocations above T_{BDT}. Initially, dislocations can form via a local transformation from the undefective lattice as pairs with opposite Burgers vectors. This is depicted in figures 1(a) and (b) of Klein and March [31]. Then, as a result of further local transformations, they can move apart. Each dislocation may be considered to be a positive-curvature disclination (say as formed by a pentagonal ring in the graphene layer) and a negative-curvature dislocation (say as associated with a heptagonal ring), such that the overall curvature of the dislocation is zero.

Klein and March [31] have also discussed in some detail the geometry associated with thermally induced structural defects in silicon: we return very briefly to this topic in section 5 immediately below.

5. Summary and possible future directions

Three widely different classes of chemically bonded materials have been treated in the present study. Starting with molecular solids, the example of solid $X(\mathrm{CH}_3)_4$: $X = \mathrm{C}$, Si or Ge, was considered in some detail in section 2 and there can be little doubt that the melting curve $T_m(p)$ of this material under pressure is importantly linked with a lower temperature phase boundary separating orientationally ordered and disordered molecular assemblies in these tetramethyls.

For the future, it would be theoretically of importance to start from the Siringo Hamiltonian [2] rather than the PK phenomenology based on equations (2.1) to (2.4) above. However, analytic work may well then need complementing by extensive computer simulation. Secondly, and again motivated by the example of solid $\mathrm{C(CH_3)_4}$ treated here, we want to emphasize the interest in other aspects of the orientational order-disorder phase transition. One of these, which shows promise of bridging two areas treated separately in the present study, is that of molecular nitrogen physisorbed on graphite. Cooling below 30 K, such an assembly is known to exhibit an orientational phase transition [35; see also 36], and further theoretical studies here are obviously highly worthwhile.

Turning to the second area, that of melting and mechanical properties of *d*-electron transition metals, important regularities are emerging from two models [15,17] which rest heavily on a mechanism of melting that is dislocation mediated. Their essential shape, as emphasized here (see also [19]), is summarized in equations (3.1) and (3.2) and a further consequence, of course approximate, is subsumed into equation (3.3), which is now structure independent. It is important, for the future, to give careful attention to getting the order of the melting transition correct: i.e. first-order, as it seems unlikely that a model with solely dislocations can do that. But more urgently, there is a need for much further work, both experimental and theoretical, on the brittle-to-ductile transition in directionally bonded transition metals. One line of progress would clearly be to follow the temperature of the BPT as a function of external pressure, say in bcc metals like Nb and W. This is especially true now that there is a lot of progress on the melting line under pressure (for theoretical progress, see Appendix 5.1).

Last, but by no means least, the covalently bonded networks of graphite and silicon deserve a lot more attention. Thus, while the melting line of graphite under pressure was measured quite recently by Togoya [37], it seems a matter of importance to decide experimentally whether there is a brittle-to-ductile transition in this sp^2 bonded material and, if so, how T_{BDT} changes under pressure. While such a transition is well established in Si, to the knowledge of the writer there have been, to date, no studies of the variation of T_{BDT} in this sp^3 bonded material with pressure and that would seem now a matter of considerable importance.

Acknowledgments

The writer wishes to acknowledge that this study was begun during a visit to the Abdus Salam International Centre for Theoretical Physics in 2004. Special thanks go to Professor V.E. Kravtsov for the stimulating atmosphere in which the work was carried out and for generous hospitality. This article was brought to fruition at DIPC, San Sebastian, in 2005 and thanks are due to Professors P.M. Echenique and A. Rubio for much encouragement and for generous hospitality. Also, the author acknowledges his indebtness to his colleagues and coauthors, Dr. C. Amovilli, Professor D.J. Klein and Dr. C.C. Matthai. Without their practical help and invaluable discussions, the results of this study could not have been achieved. Finally the author is most grateful to Professors M. Khantha and V. Vitek for valuable comments on the MS of this review.

Notes added in Proof

1. Full details of the model presented in [25] are given in M. Khantha and V. Vitek. *Acta Mater*., **45**, 4675 (1997) and KPV: ibid **45**, 4687.
2. The generalization of [25] to three dimensions, with inclusion of strain rate effects is discussed by KPV in *Mater. Sci. Eng*. A319-21, **484** (2001). Observations of the BDT temperature in several materials are also recorded there.

References

[1] V. Tozzini, N.H. March, M.P. Tosi. *Phys. Chem. Liquids*, **37**, 185 (1989).
[2] F. Siringo. *Phys. Lett*., **A226**, 378 (1997).
[3] J.A. Pople, F.E. Karasz. *J. Phys. Chem. Solids*, **18**, 28 (1961): ibid, **20**, 294 (1961).
[4] G.W. Smith. *J. Chem. Phys*., **42**, 4229 (1965).
[5] L.M. Amzel, L.N. Becka. *J. Phys. Chem. Solids*, **30**, 521 (1969).
[6] J.E. Lennard-Jones, A.F. Devonshire. *Proc. Roy. Soc. (London)*, **A169**, 317 (1939); ibid, **A170**, 464 (1939).
[7] A.R. Ubbelohde. *The Molten State of Matter*, Wiley, New York (1978).
[8] J.G. Powles, H.S. Gutowsky. *J. Chem. Phys*., **21**, 1704 (1965).
[9] R. LeSar. *J. Chem. Phys*., **86**, 4138 (1987).
[10] J.G. Kirkwood, E. Monroe. *J. Chem. Phys*., **9**, 514 (1941).
[11] T.V. Ramakrishnan, M. Yussouff. *Solid State Commun*., **21**, 389 (1977).
[12] A.D.J. Haymet, D.W. Oxtoby. *J. Chem. Phys*., **74**, 2559 (1981).
[13] N.H. March, M.P. Tosi. *Phys. Chem. Liquids*, **11**, 79 (1981).
[14] N.H. March, M.P. Tosi. *Phys. Chem. Liquids*, **11**, 129 (1981).
[15] H. Kleinert, Y. Jiang. *Phys. Lett*., **A313**, 152 (2003).
[16] A.C. Lawson, *Phil. Mag*., **81**, 255 (2001).
[17] L. Burakovsky, D.L. Preston, R.R. Silbar. *Phys. Rev*., **B61**, 15011 (2000).
[18] L. Burakovsky, C.W. Graff, D.L. Preston. *Phys. Rev*., **B67**, 094107 (2003).
[19] C.C. Matthai, N.H. March, *Phys. Chem. Liquids* (2006).
[20] A.B. Bhatia, N.H. March. *J. Chem. Phys*., **80**, 2076 (1984).
[21] P. Minchin, A. Meyer, W.H. Young. *J. Phys*., **F4**, 2117 (1974).
[22] See, for example, N.H. March, M.P. Tosi. *Introduction to Liquid State Physics*, World Scientific: Singapore (2002).
[23] R.A. Johnson. *Phys. Rev*., **B37**, 3924 (1988).
[24] See, for instance, C.W. Lung, N.H. March. *Mechanical Properties of Matter*, World Scientific, Singapore, (1997).
[25] M. Khantha, D.P. Pope, V. Vitek. *Phys. Rev. Lett*., **73**, 684 (1994).
[26] J.M. Kosterlitz, D.J. Thouless. *J. Phys*., **6**, 1181 (1973).

[27] See also the three-dimensional study of N. Gupte, S.R. Shenoy. *Phys. Rev.*, **B31**, 3150 (1985).
[28] P.B. Hirsch, S.G. Roberts. *Acta Mater.*, **44**, 2361 (1996).
[29] C. Scandian, *et al. Phys. Status Solidi*, **171**, 67 (1999).
[30] Y.Q. Sun, P.M. Hazzledine, P.B. Hirsch. *Phys. Rev. Lett.*, **88**, 065503 (2002).
[31] D.J Klein, N.H. March. *Phys. Chem. Liquids*, **42**, 545 (2004).
[32] J.S. Langer, L. Pechenik. *Phys. Rev.*, **E68**, 061507 (2003).
[33] D.J. Klein. *Phys. Chem. Phys.*, **4**, 2099 (2002).
[34] D.J. Klein. *Intl. J. Quantum. Chem.*, **95**, 600 (2003).
[35] R.D. Diehl, M.F. Toney, S.C. Fain. *Phys. Rev. Lett.*, **48**, 177 (1982).
[36] B. Hetényi, B.J. Berne. *J. Chem. Phys.*, **114**, 3674 (2001).
[37] M. Togaya. *Phys. Rev. Lett.*, **79**, 2474 (1997).
[38] N.H. March. *Phys. Chem. Liquids*, **16**, 209 (1987).
[39] N.H. March, *Phys. Rev.*, **B40**, 3356 (1989).
[40] A.S. Argon. *Acta Metall.*, **35**, 1851 (1987).
[41] H. Ledbetter. *Z. Metallkd.*, **82**, 820 (1991).
[42] H. Siethoff, K. Ahlborn. *Phys. Status Solidi*, **B190**, 179 (1995).
[43] L. Burakovsky, D.L. Preston. *J. Phys. Chem. Solids*, **65**, 1581 (2004).

Appendix 3.1: Models of monovacancy formation energy E_{IV}^{f} in terms of elastic constants

The purpose of this Appendix is to outline how other variables than the thermal energy $k_M T_m$ at melting might influence the monovacancy formation energy E_{IV}^{f} if one wishes to understand more about the fluctuations around the mean value of the ratio $E_{IV}^{f}/k_B T_m$. One indication in the main text that elastic constants might not then be sufficient information is the pair potential formula (3.4) of Bhatia and March [20]. That the bulk modulus B appears there (rather than the shear modulus G that emerges from a glue model [23] transcending pair-wise interactions, which is certainly required in *d*-electron directionally bonded transition metals) has already been noted above.

As in section 3.1, appeal will be made to the properties of the liquid just above the temperature T_m (compare equations (3.4) and (3.5)). To do this, let us invoke thermodynamics and a *Law* going back to Joule. If E is the internal energy and V the volume, the departure from Joule's Law, which states that E is independent of V, in the dense liquid resulting, say, from melting the close-packed *d*-electron metals Pd and Pt, can be estimated from thermodynamics, via the pressure equation

$$p = -\left(\frac{\partial F}{\partial V}\right)_T = -\left(\frac{\partial E}{\partial V}\right)_T + T\left(\frac{\partial S}{\partial V}\right)_T, \tag{A3.1.1}$$

in the customary thermodynamic notation. Using the Maxwell relation

$$\left(\frac{\partial S}{\partial V}\right)_T = \left(\frac{\partial p}{\partial T}\right)_V \tag{A3.1.2}$$

in equation (A3.1.1) gives immediately

$$\left(\frac{\partial E}{\partial V}\right)_T = T\left(\frac{\partial p}{\partial T}\right)_V - p. \tag{A3.1.3}$$

Using next the well-known formula for the specific heat difference $c_P - c_V$ in terms of the thermal expansion and compressibility, one reaches after a short calculation the result [38]

$$c_P - c_V = \rho\left[\frac{p}{\rho k_B T} + \frac{1}{\rho k_B T}\left(\frac{\partial E}{\partial V}\right)_T\right]^2 k_B^2 T K_T \tag{A3.1.4}$$

where ρ is here the atomic number density while K_T is the isothermal compressibility of the liquid. Recalling that for typical monoatomic liquids near the melting point, $p \ll \rho k_B T$, a quantitative expression for the departure from Joule's Law is readily extracted in the form

$$\frac{1}{\rho k_B T}\left(\frac{\partial E}{\partial V}\right)_T \simeq \left[\frac{(\gamma - 1)c_V/k_B}{S(0)}\right]^{1/2} \tag{A3.1.5}$$

where $\gamma = c_P/c_V$, and K_T has been written in terms of the long wavelength limit $S(0)$ of the liquid structure factor $S(q)$, introduced in equation (3.5), using the relation of fluctuation theory [22]

$$S(0) = \rho k_B T K_T. \tag{A3.1.6}$$

If, for convenience of presentation, we first invoke a pair potential $\phi(r)$, to be then *corrected* below, the internal energy of the liquid may be written, for $\phi(r)$ assumed density independent below, as

$$E = \frac{3}{2} N k_B T + \frac{NP}{2}\int g(r)\phi(r)\, d\mathbf{r} \tag{A3.1.7}$$

where $g(r)$ is, essentially, the Fourier transform of $S(q)$. Using again the study of Minchin *et al.* [21], one has for the vacancy formation energy

$$E_{IV}^f = -\frac{\rho}{2}\int g(r)\phi(r)\, d\mathbf{r} - k_B T \tag{A3.1.8}$$

leading to the result

$$\frac{E_{IV}^f}{k_B T_m} \simeq \left[\frac{(\gamma - 1)(c_V/k_B)}{S(0)}\right]_{T_m}^{1/2} \tag{A3.1.9}$$

where a (small) term involving the density derivative of the pair correlation function $g(r)$ in the liquid near T_m has been omitted.

The writer, in an attempt to transcend pair potential theory, has elsewhere pointed out that, for transition metals such as Pd and Pt where glue models are required, one can use Johnson's embedded atom results [23] to obtain a (weaker, of course) inequality [39]

$$\frac{E^f_{IV}}{k_B T_m} \leq \frac{5}{3}\frac{c_V}{k_B}\frac{(\gamma - 1)^{1/2}}{J\gamma}\frac{G\Omega}{k_B T_m}, \tag{A3.1.10}$$

where J is approximately constant. In the spirit of the correlations discussed in the body of the text, between $k_B T_m$, $G\Omega$ and the monovacancy formation energy, equations (A3.1.9) and (A3.1.10) indicate that *refinements* of such *average* predictions will involve the ratio of specific heats γ plus c_V/k_B also.

Appendix 3.2: Models relating brittle-to-ductile transition temperature T_{BDT} to melting temperature T_m at atmospheric pressure

In the body of the text, reference has been made to a rough empirical correlation between T_{BDT} and the melting temperature T_m. The purpose of this Appendix is to compare and contrast two attempts which have been made to model T_{BDT}.

The first of these, due to Argon [40], is a relation having the form

$$T_{\mathrm{BDT}} = \left[A + \eta\frac{T_0}{T_m}\right]^{-1} T_0. \tag{A3.2.1}$$

The term A involves an activation energy, while η is a parameter describing the temperature dependence of the shear modulus G. T_0 also involves G together with Poisson's ratio and the atomic volume of the body-centred-cubic (bcc) metals with which Argon was concerned. To compare with the second model, due to KPV [25], it will be useful to rewrite equation (A3.2.1) in the equivalent form

$$\frac{1}{T_{\mathrm{BDT}}} = \frac{1}{T_0}\left[A + \eta\frac{T_0}{T_m}\right] = \frac{\eta}{T_m} + \frac{A}{T_0} \tag{A3.2.2}$$

Argon's suggestion to take $\eta = \frac{1}{2}$ appears from equation (A3.2.2) to be the likely reason why he found, for the example of $\alpha - \mathrm{Fe}$, $T_{\mathrm{BDT}} > T_m$, whereas empirically $T_{\mathrm{BDT}} = \{275 \pm 25\}\,\mathrm{K}$ and $T_m = 1811\,\mathrm{K}$, while for another bcc metal W, $T_{\mathrm{BDT}} = \{400 \pm 50\}\,\mathrm{K}$ with $T_m = 3695\,\mathrm{K}$.

Let us now relate the general form in equation (A3.2.2) to that proposed from the Kosterlitz-Thouless-like [26, 27] modelling of KPV [25]. Prompted by equation (A3.2.2), we first take the inverse of the basic equation (6) of KPV [25]. Then we find, with β written for $(k_B T_{\mathrm{BDT}})^{-1}$

$$\beta = \frac{8\pi(1-\nu)(1 + \sigma b^2 \beta r_0/4)}{G_0 b^3[1 - 2\pi \exp(-\beta E b + \sigma b^2 \beta r_0/2)]} \tag{A3.2.3}$$

Here, G_0 denotes the shear modulus (in the absence of dislocations), b is the magnitude of the Burgers vector, while r_0 and E represent respectively the core radius and core energy of the dislocation. The final quantity, σ, appearing in equation (A3.3) is the shear stress acting on a slip plane which in KPV [25] is assumed for convenience to be coincident with the crack plane.

The first point to stress in writing the *inverse* form (A3.2.3) is that $\beta = 1/k_B T_{\mathrm{BDT}}$ has a *scale* measured by $G_0 b^3$, which is, apart from a geometrical factor, the shear modulus times the atomic volume. Returning to equation (3.2), this factor relates, in the dislocation-mediated model of melting, to the thermal energy $k_B T_m$ associated with T_m. However, according to equation (A3.2.3) this *scaling* is refined by a *two-parameter* form, one of these *parameters* being the dimensionless combination $\sigma b^2 \beta r_0$ and the other $\beta E b$. Both of these quantities, however, involve β itself, i.e. $(k_B T_{\mathrm{BDT}})^{-1}$, which one is seeking.

If β is small, corresponding to a high temperature, it is then tempting to simplify equation (A3.2.3) to find (no doubt a rough approximation for real materials) that $k_B T_{BDT} = G_0 b^3 / 8\pi(1-\nu) \propto k_B T_m$ times a lattice structure-dependent constant. If, on the other hand, it turns out that materials can be made for which $|\beta E b| \gg \sigma b^2 \beta r_0|2$, then another limit of equation (A3.2.3) becomes

$$\frac{1}{k_B T_{\mathrm{BDT}}}\left[1 - 2\pi(1-\nu)\frac{\sigma r_0}{G_0 b}\right] \propto \frac{1}{k_B T_m}. \tag{A.3.2.4}$$

It needs much fuller investigation before deciding whether either of the limiting cases of equation (A3.2.3) discussed above has a range of validity relevant for real materials. However, it may prove worthwhile, when further data is available for bcc metals beyond that quoted above for $\alpha-\mathrm{Fe}$ and W, to make a plot of $1/k_B T_{\mathrm{BDT}}$ *versus* $1/k_B T_m$, bearing in mind the forms (A3.2.2) and (A3.2.4) above. In the meantime, this Appendix should be viewed, for the *d*-electron transition metals, as modelling in different ways the interconnection stressed in the title of this article between melting temperature and a precursor cooperative phenomenon, namely the BDT.

Appendix 5.1: On the pressure dependence of the melting curve $T_m(p)$ in transition metals and its relation to the shear modulus

We take as the starting point the formula of Ledbetter [41]. This relates the Debye temperature θ_D to the shear modulus G by

$$\theta_D = \frac{C}{\Omega^{1/3}}\left(\frac{G}{\rho}\right)^{1/2}. \tag{A5.1}$$

Here, C is a constant, Ω the atomic volume while ρ denotes the density. Siethoff and Ahlborn [42] verified Ledbetter's result (A5.1) by applying it to a variety of different systems.

Combining this relation (A5.1) with the melting criterion of Lindemann [16], one is led to the relation (see also [18])

$$\frac{G(\rho, T_m(\rho))}{\rho T_m(\rho)} = \frac{G(\rho_{\mathrm{ref}} T_m(\rho_{\mathrm{ref}}))}{\rho_{\mathrm{ref}} T_m(\rho_{\mathrm{ref}})}, \tag{A5.2}$$

where ρ_{ref} denotes a chosen reference density.

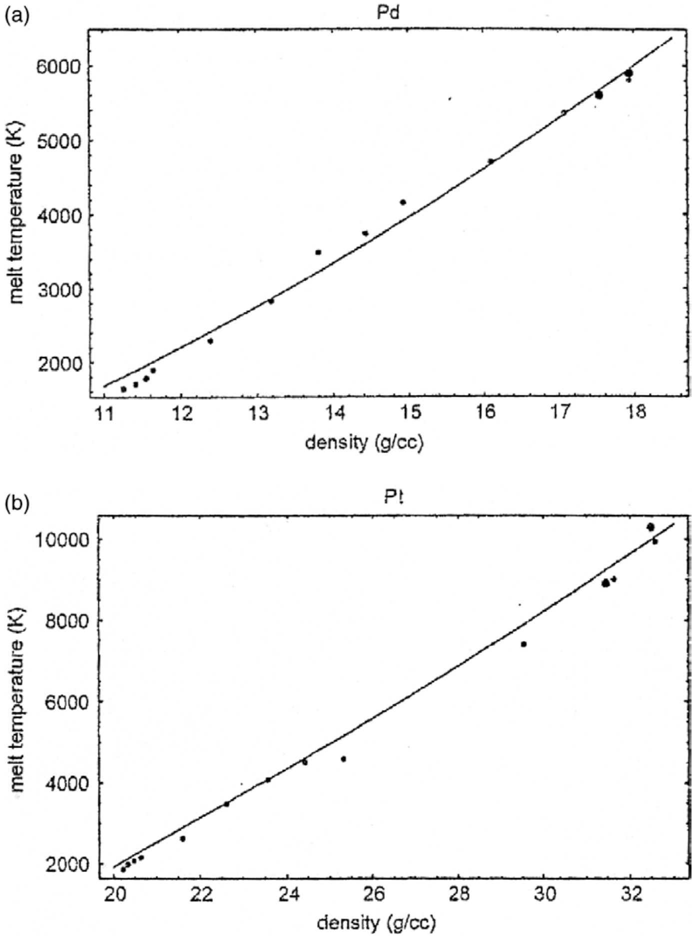

Figure A1. Shows melting curves under pressure of two *d*-electron transition metals: (a) Pd and (b) Pt. [Redrawn from Burakovsky and Preston [43].]

Because of the focus of the present result on relating melting temperature of chemically bonded solids to precursor collective phenomena, we note that Burakovsky and Preston [43] in very recent work have calculated the melting curves $T_m(\rho)$ of two *d*-electron transition metals, namely Pd and Pt. Their results are redrawn in figure A1, the upper panel (a) being appropriate for Pd and (b) for Pt. Comparison they were able to make with experiment shows that these curves represent a good average fit of the presently available measurements.

We note briefly that Burakovsky and Preston [43] model the density dependence of the Gruneisen parameter γ as

$$\gamma(\rho) = \frac{1}{2} + \frac{\gamma_1}{\rho^{1/3}} + \frac{\gamma_2}{\rho^q}, \tag{A5.3}$$

where γ_1, γ_2 and $q(>1)$ are constants. The form (A5.3) was designed to represent quantitatively the experimentally determined low-pressure form of γ, the constants in equation (A5.3) being obtained for some twenty elemental solids. Using the Lindemann criterion with the model form of γ in equation (A5.3), Burakovsky and Preston calculated melting curves as a function of density for five solids, and figure A1 shown above represents a sample of their results, redrawn from their figures 4 and 5 [43].

One can therefore have confidence that if the temperature $T_{\mathrm{BDT}}(p)$ as a function of pressure p can be measured subsequently on one or more d-electron transition metals, complementary data can be set up for the melting curve $T_m(p)$ (compare section 3.2 of the body of the text).